

Precise Timing for Multiband OFDM in a UWB System

Christian R. Berger¹, Shengli Zhou¹, Zhi Tian², Peter Willett¹

¹Department of Electrical and Computer Engineering, University of Connecticut

²Department of Electrical and Computer Engineering, Michigan Technological University

Abstract—Precise positioning is one attractive application of ultra wideband (UWB) systems. Its enormous bandwidth has generated high expectation on the spatial resolution that it could achieve. However, synchronization in the presence of dense multipath is challenging, since the first arrival is not necessarily the strongest one due to channel fading. It is unclear how high a spatial resolution can be realized in practical implementation, and how reliable it will be. We in this paper address practical synchronization algorithms for multiband OFDM UWB transmission, and analyze the performance of a maximum likelihood (ML) joint timing/channel estimation algorithm. We show that the probability of mis-timing in single band OFDM has only diversity order one. Most timing errors lie closely around the right timing, as we show that the probability of timing error equal to or greater than Δ having diversity order of $\min(\Delta, L)$, where L the number of channel taps. We reveal the benefit of frequency hopping across multiple subbands that enables an N_B -fold diversity increase in timing performance, where N_B is the number of subbands used.

I. INTRODUCTION

Thanks to its by-definition large bandwidth, Ultra Wideband (UWB) technology offers many distinct properties that are appealing to numerous applications such as short range communication, radar and imaging. Especially for ranging systems, the large time-frequency product of UWB signalling promises high time resolution. This high time resolution translates into high spatial resolution, when the positioning algorithms rely on time-of-arrival (TOA) or time-difference-of-arrival (TDOA) measurements. Though promising, positioning with UWB signalling is extremely challenging: the receiver must locate the “first arrival” in the presence of dense multipath; however, the first path is not necessarily the strongest one due to channel fading [4].

UWB signalling consists of two different formats: the first is impulse radio (IR) which uses high bandwidth analog baseband pulses to carry information, see e.g., [13], [14], [15] for overviews, and the second a multicarrier approach relying on frequency-hopped orthogonal-frequency-division-multiplexing (OFDM) in multiple subbands across the UWB spectrum [1], [10]. We are interested in the following question: *from the positioning point of view, what are the relative merits of IR and multiband OFDM?*

Reference [3] has compared the positioning capabilities of IR and multiband OFDM. However, the comparison in [3] is limited to theoretical bounds. Theoretical UWB analysis does not directly translate to practical algorithms because the difficulties in UWB systems lie primarily on the implementation side due to sampling rate constraints. It is more desirable to compare practical synchronization/timing algorithms for IR and multiband OFDM. The so-called “dirty template” method stands out as one valuable approach for timing in IR that can effectively handle dense multipath [11], [16]. The application of the “dirty template” method in positioning has been presented in [4]. No synchronization algorithms for multiband OFDM based positioning are available so far.

OFDM has been the “workhorse” for a number of broadband wireless systems, including digital audio/video broadcasting, wireless local/metropolitan area networks. The literature on OFDM synchronization is thus rich, see e.g., [8], [12], [5], [6], and references therein. However, for communication purposes, OFDM does not require precise timing. Offset in the time domain translates to phase-shift in the frequency domain, which can be estimated by pilot tones, or bypassed by differential modulations.

In this paper, we address timing for multiband OFDM. We rely on the algorithm of [8] for coarse timing to capture a data block that contains circular convolution between the channel and the OFDM data symbols. We then apply the maximum-likelihood (ML) principle for joint channel and delay estimation, similar to the approaches in [5], [6]. Our main contribution is a thorough performance analysis for timing in the presence of frequency-selective fading channels. Note that existing analytical results on OFDM synchronization largely focus on frequency-flat channels, and then extend to frequency selective channels via numerical testing [8].

Our performance results of multiband OFDM utilize analytical tools for non-coherent data detection with diversity combining [7], [9]. We find:

- 1) For single band OFDM in the presence of frequency-selective fading, the probability of mis-timing has diversity order one; that is, when plotted versus average signal-to-noise ratio (SNR) on a log-log scale, the curve becomes a straight line with slope -1 at high SNR.
- 2) For single band OFDM, the probability of timing offset equal to or larger than Δ sampling periods decreases

* Z. Tian is partially supported by NSF under grant ITR ECS-0427430; P. Willett is partially supported by Office of Naval Research.

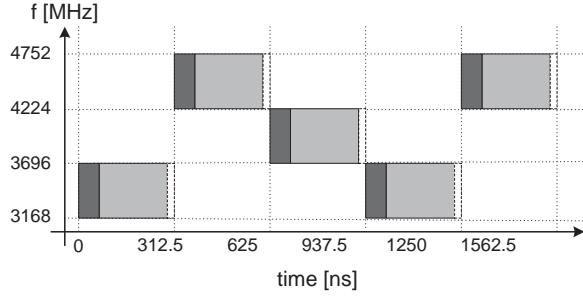


Fig. 1. Frequency hopped OFDM, including CP of 60.6 ns and switching time of 9.5 ns

with diversity order $\min(\Delta, L)$ at high SNR, where L is the number of taps of the channel.

- 3) For multiband OFDM with N_B frequency bands, the probability of mis-timing decreases with diversity order N_B at high SNR. Correspondingly, the probability of timing offset equal to or larger than Δ sampling periods decreases with diversity order $N_B \min(\Delta, L)$.

Therefore, frequency hopping over multiple bands is very effective for improving the timing accuracy of OFDM based signalling.

The rest of this paper is as follows. For single band OFDM, we present the synchronization algorithm in Section II, and carry out performance analysis in Section III. We then look into multiband OFDM synchronization in Section IV, present numerical results in Section V, and conclude in Section VI.

II. SINGLE BAND OFDM SYNCHRONIZATION

Information symbols are partitioned into blocks of length N_c , where N_c is the number of subcarriers in OFDM. The transmitter converts each data vector of length N_c , denoted by $\mathbf{s} = [s_0 \cdots s_{N_c-1}]^T$, to the corresponding OFDM symbol $\mathbf{x} = \mathbf{F}^H \mathbf{s}$ via inverse Fourier transform, where \mathbf{F} is the discrete Fourier transform (DFT) matrix of dimension $N_c \times N_c$,

$$[\mathbf{F}]_{l,k} = \frac{1}{\sqrt{N_c}} \exp\left(-j2\pi \frac{lk}{N_c}\right), \quad l, k = 0, \dots, N_c - 1, \quad (1)$$

and $(\cdot)^H$ denotes the Hermitian transpose. Cyclic prefixes (CP), which are simply the last N_g samples of the OFDM block, are inserted before each OFDM symbol as an guard interval; see the shaded dark-grey area in Fig. 1.

Multiband OFDM splits the whole UWB spectrum into multiple subbands, and adopts frequency hopped OFDM transmission across the subbands. For example, the multiband OFDM in [1] uses subbands of 528 MHz each, and the hopping is done on an OFDM symbol-by-symbol basis. The number of carriers is $N_c = 128$ and an $N_g = 32$ CP leads to a symbol length of 303 ns. Fig. 1 depicts the multiband OFDM transmission, and also considers a transmitter switching time of 9.5 ns during frequency hopping.

We use the algorithm of [8] for coarse synchronization. Our objective is to develop a fine synchronization algorithm for much improved synchronization performance. To be mathematically rigorous, we will adopt several assumptions.

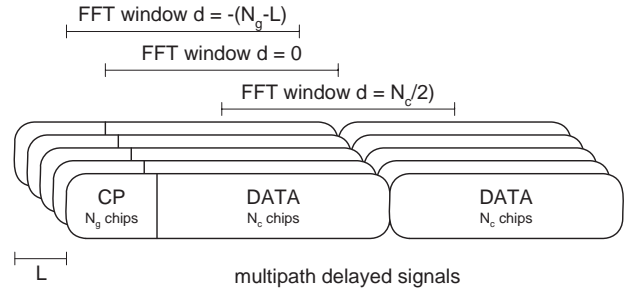


Fig. 2. Coarse synchronization in the presence of multipath

Assumption 1 *The discrete-time frequency selective channel has L taps, contained in the channel vector $\mathbf{h} := [h_0, \dots, h_{L-1}]^T$. The number of taps L is known at the receiver.*

The number of channel taps could be known a priori relying on channel models, or jointly estimated with the channel itself, as in [5].

Assumption 2 *The coarse synchronization algorithm [8] yields a delay estimate $d \in [-(N_g - L), \frac{1}{2}N_c]$.*

With L channel taps, the coarse synchronization will return delay estimates centered around $-\frac{1}{2}(N_g - L)$ [8].

After coarse synchronization, the receiver takes a received vector \mathbf{y} of length N_c starting at d , as illustrated in Fig. 2. With assumption 2, the block \mathbf{y} contains a cyclic convolution between the channel vector \mathbf{h} and the transmitted symbol block \mathbf{x} ; thus all subcarriers stay orthogonal. If $d < -(N_g - L)$, the vector \mathbf{y} does not contain a true cyclic convolution of \mathbf{h} and \mathbf{x} , although the synchronization algorithm will still work in practice. If $d > N_c/2$, the vector \mathbf{y} contains more contribution from the second OFDM symbol, which is not desirable. We further assume:

Assumption 3 *Carrier frequency offset (CFO) can be ignored, or, has been compensated already in the received sequence¹.*

Define an $N_c \times N_c$ circular shift matrix \mathbf{J}

$$\mathbf{J} = \begin{bmatrix} \mathbf{0}_{1 \times (N_c-1)} & 1 \\ \mathbf{I}_{(N_c-1)} & \mathbf{0}_{(N_c-1) \times 1} \end{bmatrix},$$

and an $N_c \times L$ zero-insertion matrix

$$\mathbf{T} = \begin{bmatrix} \mathbf{I}_L \\ \mathbf{0}_{(N_c-L) \times L} \end{bmatrix},$$

We can then represent a circular shift of \mathbf{h} with delay d as:

$$\mathbf{J}^d \mathbf{T} \mathbf{h} = \begin{bmatrix} \mathbf{0}_{1 \times d} & \mathbf{h}^T & \mathbf{0}_{1 \times (N_c-d-L)} \end{bmatrix}^T. \quad (2)$$

Define a circulant matrix

$$\mathbf{X} = [\mathbf{x}, \mathbf{J}\mathbf{x}, \dots, \mathbf{J}^{N_c-1}\mathbf{x}]. \quad (3)$$

¹CFO issues are addressed in the journal version of this paper [2].

With Assumptions 1–3, we can represent \mathbf{y} explicitly as

$$\mathbf{y} = \mathbf{X}\mathbf{J}^d\mathbf{T}\mathbf{h} + \mathbf{w}, \quad (4)$$

where \mathbf{w} contains the additive white Gaussian noise (AWGN) with variance N_0 .

Treating \mathbf{h} and d as deterministic unknowns and \mathbf{X} is training data, the received vector \mathbf{y} is Gaussian distributed with mean $\mathbf{X}\mathbf{J}^d\mathbf{T}\mathbf{h}$ and covariance matrix $N_0\mathbf{I}_{N_c}$. The likelihood function is:

$$\Lambda(\mathbf{y}; \mathbf{h}, d) = \frac{1}{(\pi N_0)^{N_c}} \cdot \exp \left\{ -\frac{1}{N_0} (\mathbf{y} - \mathbf{X}\mathbf{J}^d\mathbf{T}\mathbf{h})^H (\mathbf{y} - \mathbf{X}\mathbf{J}^d\mathbf{T}\mathbf{h}) \right\}. \quad (5)$$

Therefore, the joint maximum likelihood (ML) estimation of channel \mathbf{h} and delay d reduces to a least squares (LS) solution:

$$(\hat{d}, \hat{\mathbf{h}}) = \arg \min_{d, \mathbf{h}} \|\mathbf{y} - \mathbf{X}\mathbf{J}^d\mathbf{T}\mathbf{h}\|^2. \quad (6)$$

Define the $N_c \times L$ matrix $\mathbf{A}(d) := \mathbf{X}\mathbf{J}^d\mathbf{T}$. Assume that d is known, the ML estimate for \mathbf{h} is:

$$\hat{\mathbf{h}}(d) = (\mathbf{A}(d)^H \mathbf{A}(d))^{-1} \mathbf{A}(d)^H \mathbf{y}. \quad (7)$$

Substituting (7) into (6), the ML estimate of d becomes

$$\hat{d} = \arg \max_d \mathbf{y} \mathbf{A}(d) (\mathbf{A}(d)^H \mathbf{A}(d))^{-1} \mathbf{A}(d)^H \mathbf{y}. \quad (8)$$

We next further simplify (8) by specifying the training sequence design. To this end, we assume that

Assumption 4 All entries of the training sequence \mathbf{s} are drawn from a signal constellation with unit amplitude, e.g., phase-shift-keying (PSK) modulation.

Because any circulant matrix can be diagonalized by the DFT matrices, $\mathbf{X} = \mathbf{F}^H \text{diag}\{\sqrt{N_c}\mathbf{s}\}\mathbf{F}$, assumption 4 leads to

$$\mathbf{X}^H \mathbf{X} = N_c \mathbf{I}_{N_c}. \quad (9)$$

Thus, any sequence with a flat spectrum has perfect autocorrelation, a property shown in [17]. Based on (9), we obtain $\mathbf{A}(d)^H \mathbf{A}(d) = \mathbf{T}^H \mathbf{J}^{-d} \mathbf{X}^H \mathbf{X} \mathbf{J}^d \mathbf{T} = N_c \mathbf{I}_L$, and (8) reduces to

$$\hat{d} = \arg \max_d \|\mathbf{T}^H \mathbf{J}^{-d} \mathbf{X}^H \mathbf{y}\|^2. \quad (10)$$

Define a tentative channel estimate of length N_c as:

$$\tilde{\mathbf{h}} := \frac{1}{N_c} \mathbf{X}^H \mathbf{y} = \frac{1}{\sqrt{N_c}} \mathbf{F}^H \text{diag}\{\mathbf{s}^H\} \mathbf{F} \mathbf{y}. \quad (11)$$

To estimate d , we simply pick a length L sub-vector of $\tilde{\mathbf{h}}$ by multiplying it with the sliding window $\mathbf{T}^H \mathbf{J}^{-d}$ at delay d , and see which one has the maximum norm; i.e.,

$$\hat{d} = \arg \max_d \|\mathbf{T}^H \mathbf{J}^{-d} \tilde{\mathbf{h}}\|^2 \quad (12)$$

$$= \arg \max_d \sum_{k=d}^{d+L-1} |\tilde{h}_k|^2, \quad (13)$$

and $d \in (-\frac{1}{2}N_c, \frac{1}{2}N_c]$, where the index d to $d+L-1$ should be interpreted as $d \bmod N_c$ and $(d+L-1) \bmod N_c$. The estimation of d in (13) becomes a detection problem, to decide which L -sample segment of $\tilde{\mathbf{h}}$ has the largest energy.

In summary, single band OFDM synchronization consists of the following steps,

- Use coarse synchronization to capture a received vector \mathbf{y} of length N_c that consists of a circular convolution of the channel and the transmitted data block.
- Compute the FFT of \mathbf{y} , phase compensation in the frequency domain via multiplication with the complex conjugate of training symbols, and then go back to the time-domain with the IFFT, that renders $\tilde{\mathbf{h}}$; c.f. (11).
- Take the square of all entries of $\tilde{\mathbf{h}}$ and find the maximum energy capture by using a length L sliding window; c.f. (13).

III. TIMING PERFORMANCE ANALYSIS

For ease of presentation, we adopt the following assumption in this paper:

Assumption 5 The channel coefficients are independent and identically distributed (i.i.d.) according to a complex Gaussian distribution with zero mean and variance $1/L$; i.e., $h_l \sim \mathcal{CN}(0, 1/L)$, $l = 0, \dots, L-1$.

Our performance analysis steps also apply to other distributions, as will be commented later on.

Substituting (4) into (11), we have:

$$\begin{aligned} \tilde{\mathbf{h}} &= \frac{1}{N_c} \mathbf{X}^H (\mathbf{X}\mathbf{J}^d\mathbf{T}\mathbf{h} + \mathbf{w}) \\ &= \mathbf{J}^d\mathbf{T}\mathbf{h} + \tilde{\mathbf{w}} \\ &= [\tilde{w}_0, \dots, h_0 + \tilde{w}_d, \dots, h_{L-1} + \tilde{w}_{d+L-1}, \dots, \tilde{w}_{N_c-1}]^T \end{aligned} \quad (14)$$

where the noise vector $\tilde{\mathbf{w}} = \sqrt{N_c}^{-1} \mathbf{F}^H \text{diag}\{\mathbf{s}^H\} \mathbf{F} \mathbf{w}$ remains white but with variance N_0/N_c .

We first study pairwise error probability with a wrong decision $\hat{d} = d + \nu$, defined as:

$$\text{PEP}(\nu) = \Pr \left\{ \sum_{k=d}^{d+L-1} |\tilde{h}_k|^2 < \sum_{k=d+\nu}^{d+\nu+L-1} |\tilde{h}_k|^2 \right\}. \quad (15)$$

Depending on the value of ν , many common terms in the right hand side of (15) can be cancelled. Let us start from $\nu = 1$:

$$\text{PEP}(1) = \Pr \left\{ |\tilde{h}_d|^2 < |\tilde{h}_{d+L}|^2 \right\}. \quad (16)$$

This corresponds to non-coherent detection in a fading channel [7], where \tilde{h}_d contains both ‘‘signal’’ and noise with variance $1/L + N_0/N_c$, while \tilde{h}_{d+L} contains only noise with variance N_0/N_c . Define $x = |\tilde{h}_d|^2$ and $y = |\tilde{h}_{d+L}|^2$. Due to assumption 5 and (14), x and y are independent and Rayleigh distributed, with moments $\sigma_x^2 = (1/L + N_0/N_c)$ and $\sigma_y^2 = N_0/N_c$,

respectively. Thus

$$\begin{aligned} \text{PEP}(1) &= \Pr \{x < y\} = \int_{-\infty}^{\infty} f_Y(y) \int_{-\infty}^y f_X(x) dx dy \\ &= \frac{\sigma_y^2}{\sigma_x^2 + \sigma_y^2} \\ &= \frac{1}{2 + N_c \bar{\gamma}/L}, \end{aligned} \quad (17)$$

where we define average SNR as $\bar{\gamma} = 1/N_0$.

We now look at the general case with timing offset $1 \leq \nu \leq L$. Cancelling out common terms in (15), we obtain

$$\text{PEP}(\nu) = \Pr \left\{ \sum_{k=d}^{d+\nu-1} |\tilde{h}_k|^2 < \sum_{k=d+L}^{d+\nu+L-1} |\tilde{h}_k|^2 \right\}, \quad (18)$$

with $1 \leq \nu \leq L$. This is the error probability of non-coherent detection with receiver diversity combining over ν branches [7]. Thus, we obtain from of [7, eq. (14.4-15)]:

$$\begin{aligned} \text{PEP}(\nu) &= \\ &= \frac{1}{(2 + N_c \bar{\gamma}/L)^\nu} \sum_{k=0}^{\nu-1} \binom{\nu-1+k}{k} \left(\frac{1 + N_c \bar{\gamma}/L}{2 + N_c \bar{\gamma}/L} \right)^k, \end{aligned} \quad (19)$$

with $1 \leq \nu \leq L$, which includes (17) as a special case when $\nu = 1$.

Now we look at $\text{PEP}(\nu)$ with $\nu > L$. Since the sliding window is of length L , we infer that

$$\text{PEP}(\nu) = \text{PEP}(L), \quad L < \nu < N_c/2. \quad (20)$$

We can derive PEP in a similar fashion when ν is negative. Thanks for assumption 5, all channel taps are i.i.d., and thus

$$\text{PEP}(\nu) = \text{PEP}(|\nu|), \quad \nu < 0. \quad (21)$$

Eqns. (17), (19), (20), and (21) fully characterize all pairwise error events. These can be used for assessing the overall system performance. But first, we would like to comment on the diversity order of the PEP. At high SNR $\bar{\gamma} \gg 1$, we simplify (19) as [7, eq. (14.4-18)]:

$$\text{PEP}(\nu) \approx \binom{2\nu-1}{\nu} \left(\frac{N_c}{L} \bar{\gamma} \right)^{-\nu}, \quad 1 \leq \nu \leq L. \quad (22)$$

Therefore, $\text{PEP}(\nu)$ has diversity order ν for $|\nu| \leq L$; i.e., when plotting $\text{PEP}(\nu)$ versus SNR on a log-log scale, this curve becomes a straight line with slope $-\nu$. Diversity order is one important performance indicator, as it specifies how fast the performance improves as SNR increases. Fig. 3 depicts the PEP for several ν values, which shows the correct diversity order.

Based on PEP analysis, we now apply the union bound to assess the system performance. We have the following results:

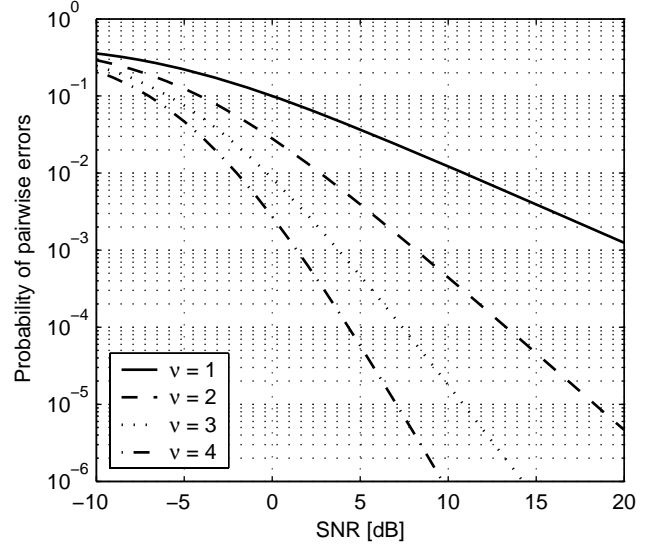


Fig. 3. Pairwise error probabilities; $L = 16$ and $N_c = 128$

Proposition 1 With assumptions 1-5, the probability of mis-timing after fine synchronization is upper bounded by

$$\begin{aligned} \Pr(\hat{d} \neq d) &\leq \sum_{\nu=-N_c/2; \nu \neq 0}^{N_c/2} \text{PEP}(\nu) \\ &= 2 \sum_{\nu=1}^L \text{PEP}(\nu) + (N_c - 2L)\text{PEP}(L), \end{aligned} \quad (23)$$

where $\text{PEP}(\nu)$ is readily computable from (19). At high SNR, the probability of mis-timing has only diversity order one.

Proposition 2 With assumptions 1-5, the probability of timing offset equal to or larger than Δ is upper bounded by

$$\begin{aligned} \Pr(|\hat{d} - d| \geq \Delta) &\leq \sum_{\nu=-N_c/2; |\nu| \geq \Delta}^{N_c/2} \text{PEP}(\nu) \\ &= \begin{cases} 2 \sum_{\nu=\Delta}^L \text{PEP}(\nu) + (N_c - 2L)\text{PEP}(L), & \Delta \leq L \\ (N_c - 2\Delta)\text{PEP}(L) & \Delta > L. \end{cases} \end{aligned} \quad (24)$$

where $\text{PEP}(\nu)$ is readily computable from (19). At high SNR, the probability of timing offset equal to or larger than Δ has diversity order $\min(\Delta, L)$.

Remark 1: We have used the i.i.d. Rayleigh fading model to derive our performance results. However, closed-form results are available for many other fading channels, because PEP is linked to the performance of non-coherent detection with diversity combining. The performance results for non-coherent equal-gain combining in [9, chapter 9.4] can now be used to replace the $\text{PEP}(\nu)$ in (19). Results are available for Rician, Nakagami fading models or any other combination of fading channels for which the moment generating function (MGF) approach is applicable.

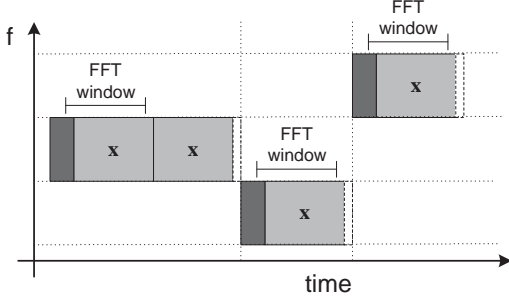


Fig. 4. Transmitted signals for multiband OFDM synchronization

IV. MULTIBAND OFDM SYNCHRONIZATION

Multiband OFDM uses fast frequency hopping across N_B different frequency bands. We assume:

Assumption 6 Channel vectors on different frequency bands, $\mathbf{h}_1, \dots, \mathbf{h}_{N_B}$, are uncorrelated.

This assumption is very reasonable given the large bandwidth of each subband in UWB systems. The delay on the first path would be the same at different frequency bands, as it is associated with the line-of-sight propagation. As revealed by Proposition 1, the probability of mis-timing has only diversity order one due to channel fading, if one subband is used. Intuitively speaking, when the first channel tap in one subband experiences deep fading, it is unlikely that the first taps on other subbands suffer from deep fading simultaneously. Hence, enhanced diversity is available if synchronization is jointly done across all used subbands. This is along the same principle as diversity reception in data communications for improved fading resistance [7].

As shown in Fig. 4, we use two identical OFDM symbols for coarse synchronization, which is not needed in subsequent frequency subbands. As the coarse synchronization usually returns a delay estimate around $-(N_g - L)/2$, a typical data collection window is also depicted in Fig. 4. Let \mathbf{y}_i denote the received vector from the i th subband. With assumptions 1-4, we have the joint likelihood function as:

$$\Lambda(\mathbf{y}_1, \dots, \mathbf{y}_{N_B}; \mathbf{h}_1, \dots, \mathbf{h}_{N_B}, d) = \frac{1}{(\pi N_0)^{N_B N_c}} \cdot \exp \left\{ -\frac{1}{N_0} \sum_{i=1}^{N_B} [\mathbf{y}_i - \mathbf{XJ}^d \mathbf{T} \mathbf{h}_i]^H [\mathbf{y}_i - \mathbf{XJ}^d \mathbf{T} \mathbf{h}_i] \right\}. \quad (25)$$

Due to AWGN assumption, the ML solution becomes

$$(\hat{d}, \hat{\mathbf{h}}_1, \dots, \hat{\mathbf{h}}_{N_B}) = \arg \min_{d, \{\mathbf{h}_i\}} \sum_{i=1}^{N_B} \|\mathbf{y}_i - \mathbf{XJ}^d \mathbf{T} \mathbf{h}_i\|^2. \quad (26)$$

Following the steps in Section II, we define

$$\tilde{\mathbf{h}}_i = \frac{1}{\sqrt{N_c}} \mathbf{F}^H \text{diag}\{\mathbf{s}^H\} \mathbf{F} \mathbf{y}_i. \quad (27)$$

The ML estimation for d is

$$\begin{aligned} \hat{d} &= \arg \max_d \sum_{i=1}^{N_B} \|\mathbf{T}^H \mathbf{J}^{-d} \tilde{\mathbf{h}}_i\|^2 \\ &= \arg \max_d \sum_{i=1}^{N_B} \sum_{k=d}^{d+L-1} |\tilde{h}_{i,k}|^2 \end{aligned} \quad (28)$$

which combines the energy of channel estimates from all branches to decide the best estimate of d . With Assumption 5 on each subband, the pairwise error probability events can be similarly calculated as

$$\begin{aligned} \text{PEP}(\nu) &= \Pr \left\{ \sum_{k=d}^{d+\nu-1} \sum_{i=1}^{N_B} |\tilde{h}_{i,k}|^2 < \sum_{k=d+L}^{d+\nu+L-1} \sum_{i=1}^{N_B} |\tilde{h}_{i,k}|^2 \right\} = \\ &= \frac{1}{(2 + N_c \bar{\gamma}/L)^{\nu N_B}} \sum_{k=0}^{\nu N_B - 1} \binom{\nu N_B - 1 + k}{k} \left(\frac{1 + N_c \bar{\gamma}/L}{2 + N_c \bar{\gamma}/L} \right)^k \end{aligned} \quad (29)$$

with $\forall 1 \leq \nu \leq L$. Eq. (29) corresponds to non-coherent detection with diversity combing of νN_B branches. We can simply plug (29) into (23) for the union bound on the probability of mistiming, and into (24) for the union bound on the probability of timing offset equal to or larger than Δ . In summary, we have:

Proposition 3 With assumption 1-6, the union bound on the probability of mistiming in multiband OFDM is (23), with the pairwise error probability computed in (29). Correspondingly, the union bound on the probability of timing offset equal to or larger than Δ is (24) with the pairwise error probability computed in (29). At high SNR, the probability of mistiming in multiband OFDM has diversity order of N_B , while the probability of timing offset equal to or larger than Δ has diversity order of $N_B \min(\Delta, L)$.

Therefore, multiband OFDM enhances the timing performance by an N_B -fold diversity increase. Timing precision can be considerably improved via frequency hopping over multiple bands.

V. NUMERICAL RESULTS

We simulate the coarse synchronization from [8] followed by the fine timing from section II. The system parameters are $N_c = 128$, $N_g = 32$, as in [1]. The channel length is set to $L = 16$, and the channel taps are i.i.d. Rayleigh distributed. The Monte Carlo simulations use 10^6 runs.

A. Single Band Results

Fig. 5 shows the probability of timing offset equal to or larger than Δ after fine synchronization. It shows how an increasing part of the errors accumulate around the right timing, as the probability of having a timing error of Δ or more decreases with diversity Δ . We would like to point out that the union bounds included in the graph are only true bounds for high SNR, since they were derived using assumption 2 - which does not hold true for low SNRs; but even for low SNRs, the bounds are close to the simulated performance.

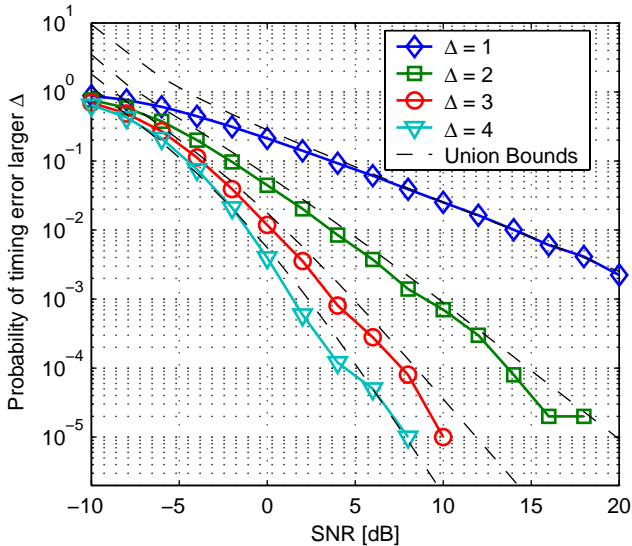


Fig. 5. Probability of timing error equal to or greater than Δ for single band OFDM synchronization

B. Multiband Results

The multiband simulation uses two identical symbols on one frequency band for coarse synchronization and only one symbol on other frequency bands. After diversity combining, the probability of mis-timing decreases with diversity N_B and converge nicely against the theoretical union bounds, as shown in Fig. 6.

VI. CONCLUSIONS

We addressed synchronization issues for multiband OFDM UWB transmissions in the presence of frequency selective channels. We analyzed the timing performance, relying on results from non-coherent data communication in fading channels. We showed that the probability of mis-timing was upper bounded by a diversity-one event, but most timing errors lie closely around the right timing, with the probability of timing error equal to or greater than Δ having diversity order of $\min(\Delta, L)$, where L the number of channel taps. We further showed that frequency hopping across multiple subbands considerably improves the timing performance with N_B -fold diversity increase, where N_B is the number of subbands used.

In future work, we would like to compare practical synchronization algorithms between impulse radio (IR) and multiband OFDM UWB transmissions.

REFERENCES

- [1] A. Batra, J. Balakishnan, G. R. Aiello, J. R. Foerster, and A. Dabak, "Design of a multiband OFDM system for realistic UWB channel environments," *IEEE Transactions on Microwave Theory and Techniques*, vol. 52, no. 9, pp. 2123–2138, Sept. 2004.
- [2] C. R. Berger, S. Zhou, Z. Tian, and P. Willett, "Precise timing for multiband OFDM in a UWB system," *IEEE Trans. Commun.*, to be submitted.
- [3] R. Cardinali, L. De Nardis, P. Lombardo, and M.-G. Benedetto, "UWB ranging accuracy for applications within IEEE 802.15.3a," *Networking with UWB 2005. 2nd International Workshop*, pp. 65–69, July 2005.

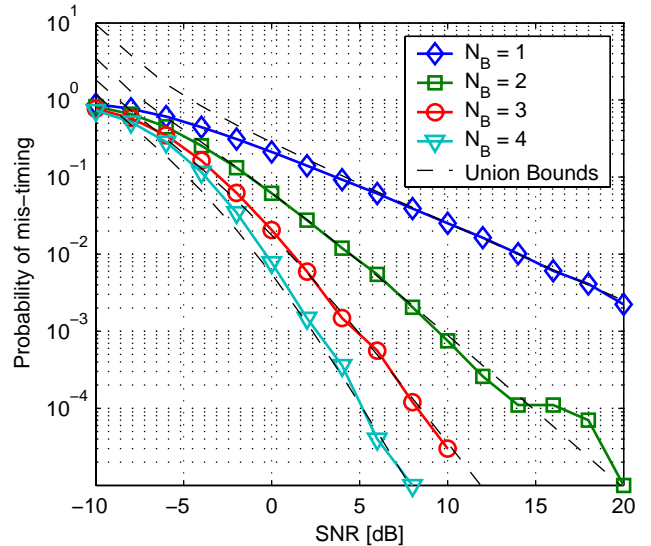


Fig. 6. Probability of mistiming for multiband OFDM synchronization

- [4] S. Gezici, Z. Tian, G. B. Giannakis, H. Kobayashi, A. Molisch, V. Poor, and Z. Sahinoglu, "Localization via ultra-wideband radios - a look at positioning aspects of future sensor networks," *IEEE Trans. Signal Processing*, vol. 22, no. 4, pp. 70–84, July 2005.
- [5] E. G. Larsson, G. Liu, J. Li, and G. B. Giannakis, "Joint symbol timing and channel estimation for OFDM based WLANs," *IEEE Communications Letters*, vol. 5, no. 8, pp. 325–327, Aug. 2001.
- [6] W. C. Lim, B. Kannan, and T. T. Tjhung, "Joint channel estimation and OFDM synchronization in multipath fading," in *Proc. of International Conference on Communications*, 2004, pp. 983–987.
- [7] J. G. Proakis, *Digital Communications*, McGraw-Hill, New York, 4 edition, 2001.
- [8] T. M. Schmidl and D. C. Cox, "Robust frequency and timing synchronization for OFDM," *IEEE Trans. Commun.*, vol. 45, no. 12, pp. 1613–1621, Dec. 1997.
- [9] M. K. Simon and M.-S. Alouni, *Digital Communication over Fading Channels*, Wiley, New York, 2000.
- [10] W. P. Siritwongpairat, W. Su, M. Olfat, and K. J. R. Liu, "Multiband-OFDM MIMO coding framework for UWB communication systems," *IEEE Trans. Signal Processing*, vol. 54, no. 1, pp. 214–224, Jan. 2006.
- [11] Z. Tian and G. B. Giannakis, "A GLRT approach to data-aided timing acquisition in UWB radios - Part I: Algorithms," *IEEE Trans. Wireless Commun.*, vol. 4, no. 6, pp. 2956–2967, Nov. 2005.
- [12] J. J. van de Beek, M. Sandell, and P. O. Borjesson, "ML estimation of time and frequency offset in OFDM systems," *IEEE Trans. Signal Processing*, vol. 45, no. 7, pp. 1800–1805, July 1997.
- [13] M. Z. Win and R. A. Scholtz, "Impulse radio: How it works," *IEEE Communications Letters*, vol. 2, no. 2, pp. 36–38, Feb. 1998.
- [14] M. Z. Win and R. A. Scholtz, "Ultra-wide bandwidth time-hopping spread-spectrum impulse radio for wireless multiple-access communications," *IEEE Trans. Commun.*, vol. 48, no. 4, pp. 679–689, Apr. 2000.
- [15] L. Yang and G. B. Giannakis, "Ultra-wideband communications: An idea whose time has come," *IEEE Trans. Signal Processing*, vol. 21, no. 6, pp. 26–54, Nov. 2004.
- [16] L. Yang and Georgios B. Giannakis, "Timing ultra-wideband signals with dirty templates," *IEEE Trans. Commun.*, vol. 53, no. 11, pp. 1952–1963, Nov. 2005.
- [17] S. Zhou, G. B. Giannakis, and A. Swami, "Digital multi-carrier spread spectrum versus direct sequence spread spectrum for resistance to jamming and multipath," *IEEE Trans. Commun.*, vol. 50, no. 4, pp. 643–655, Apr. 2002.